Signatures of the Self-Similar Regime of Strongly Coupled Stimulated Brillouin Scattering for Efficient Short Laser Pulse Amplification

L. Lancia,[1,2,*] A. Giribono,[1,2] L. Vassura,[3,1] M. Chiaramello,[4] C. Riconda,[4] S. Weber,[5] A. Castan,[6] A. Chatelain,[3] A. Frank,[7] T. Gangolf,[8,6] M. N. Quinn,[9] J. Fuchs,[3] and J.-R. Marquès[3]

[1]*Dipartimento SBAI, Università di Roma "La Sapienza," Via Antonio Scarpa 14, 00161 Rome, Italy*
[2]*INFN–Sezione Roma 1–SAPIENZA, University of Rome, 00185 Rome, Italy*
[3]*LULI–CNRS, École Polytechnique, CEA: Université Paris-Saclay; UPMC Université Paris 06: Sorbonne Universités, F-91128 Palaiseau cedex, France*
[4]*LULI–UPMC Université Paris 06: Sorbonne Universités; CNRS, Ecole Polytechnique, CEA: Université Paris-Saclay, F-75252 Paris cedex 05, France*
[5]*Institute of Physics of the ASCR, ELI–Beamlines, 18221 Prague, Czech Republic*
[6]*LULI–CEA, CNRS, École Polytechnique: Université Paris-Saclay; UPMC Université Paris 06: Sorbonne Universités, F-91128 Palaiseau cedex, France*
[7]*GSI Helmholtzzentrum für Schwerionenforschung GmbH, 64291 Darmstadt, Germany*
[8]*ILPP, Heinrich-Heine Universität Düsseldorf, 40225 Düsseldorf, Germany*
[9]*IZEST, CEA, École Polytechnique, F-91128 Palaiseau cedex, France*

(Received 12 August 2015; published 16 February 2016)

Plasma-based laser amplification is considered as a possible way to overcome the technological limits of present day laser systems and achieve exawatt laser pulses. Efficient amplification of a picosecond laser pulse by stimulated Brillouin scattering (SBS) of a pump pulse in a plasma requires to reach the self-similar regime of the strongly coupled (SC) SBS. In this Letter, we report on the first observation of the signatures of the transition from linear to self-similar regimes of SC-SBS, so far only predicted by theory and simulations. With a new fully head-on collision geometry, subpicosecond pulses are amplified by a factor of 5 with energy transfers of few tens of mJ. We observe pulse shortening, frequency spectrum broadening, and down-shifting for increasing gain, signatures of SC-SBS amplification entering the self-similar regime. This is also confirmed by the power law dependence of the gain on the amplification length: doubling the interaction length increases the gain by a factor 1.4. Pump backward Raman scattering (BRS) on SC-SBS amplification has been measured for the first time, showing a strong decrease of the BRS amplitude and frequency bandwidth when SBS seed amplification occurs.

DOI: 10.1103/PhysRevLett.116.075001

Plasma amplification [1] is a part of the growing field of plasma optics [2], which aims at manipulating light (amplifying, focusing, diffracting, etc.) using a fully ionized plasma. This approach is expected to open up ways to reach exawatt laser pulses. Such power, and the attainable intensity, will allow exploring new physical regimes of laser-matter interaction, and thus unfold new possibilities in the investigation of fundamental and applied physics [3]. The technological limits, in terms of damage threshold [4] of optical components and the occurrence of nonlinearities, that undermine the use of solid-state based technologies [chirped-pulse amplification (CPA) or optical parametric chirped-pulse amplification (OPCPA) [5,6]] for the production of ultrahigh intensities, can indeed be overcome by the damageless nature of a plasma as an amplifying medium. A plasma amplifier is a single pass amplification process that features a unidirectional energy transfer from a long, energetic, and moderate-intensity pump electromagnetic wave ($\boldsymbol{k}_p$, ω_p), to a shorter and less energetic seed one ($\boldsymbol{k}_s$, ω_s). The underlying physical mechanism is based on the response of the plasma ($\boldsymbol{k}_{\rm pl}$, $\omega_{\rm pl}$) to the intense laser excitation, which fulfils the energy and momentum conservation in the wave coupling: $\omega_p = \omega_s + \omega_{\rm pl}$ and $\boldsymbol{k}_p = \boldsymbol{k}_s + \boldsymbol{k}_{\rm pl}$. In general, the modes characterizing the plasma response can be classified as electron plasma waves (stimulated Raman amplification, SRA) [6,7] or ion acoustic waves (stimulated Brillouin amplification, SBA). Because of the faster response of an electron plasma wave, SRA has been initially more investigated theoretically and experimentally [7–10] for amplification of subpicosecond laser pulses. One of the saturation mechanisms of SRA is the electron plasma wave breaking, limiting the maximum pump intensity [11,12]. Achieving high energy transfers then requires large transverse beam sizes and thus, because of the required frequency-matching conditions, homogeneous plasmas over a large interaction volume. Therefore, more attention has been recently directed towards SBA, in particular towards its strongly coupled (SC) SBA limit [13–22]. This is not based on the excitation of proper ion acoustic modes (ion waves) of the plasma, but on intensity-driven low-frequency modes. The frequency $\omega_{\rm SC}$ of this forced ion mode [23] can be written as

$$\frac{\omega_{SC}}{\omega_0} \simeq 0.0037(1+i\sqrt{3})\left[\frac{Z^*}{A}\frac{n_e}{n_c}\left(1-\frac{n_e}{n_c}\right)I_{15}\lambda_\mu^2\right]^{1/3}. \quad (1)$$

Here, Z^*, A, n_e, I_{15}, λ_μ, $n_c \simeq 10^{21}/\lambda_\mu^2$ are, respectively, ion charge, mass numbers, electron plasma density, laser intensity in units of 10^{15} W/cm^2, laser wavelength expressed in microns, and critical density. The threshold condition for accessing this quasimode regime is given by Eq. (2) in [21]. These nonlinear oscillations (i) set a fast (~100 fs) energy transfer, suited for the amplification of short pulses, (ii) can sustain pump intensities [22] several orders of magnitude higher than SRA, and (iii) present a frequency $\omega_{SC} \ll \omega_p$ [see Eq. (1)] such that no frequency down-shift of one pulse with respect to the other is needed to fulfil the electromagnetic coupling. A natural spread of frequencies is provided either by the shortness of the pulse or by the fact that the ion-acoustic mode has a growth rate comparable to the frequency [Eq. (1)]. Since no frequency-matching condition is necessary, SC-SBA does not require a homogeneous plasma.

The linear regime of SC-SBA is characterized by negligible pump losses. The seed grows exponentially, at a rate given by $\gamma_{SC} \equiv \Im(\omega_{SC})$, maximized if the frequency of the backscattered or amplified wave is down-shifted by $\Re(\omega_{SC})$. This growth is accompanied by a temporal stretching of the pulse. To be efficient, SC-SBA needs to enter the self-similar regime [13,24], where non-negligible energy transfer and pulse compression occur. Other signatures of this regime are a significant and nonsymmetric broadening of the frequency spectrum (in addition to the down-shift in the linear regime), and the amplitude growing as a power law of the amplification length.

It was recently demonstrated [17] that energy transfer from a long to a short (subpicosecond) pulse via the SC stimulated Brillouin scattering (SBS) mechanism is possible. However, in that experiment, the beam overlap, hence the energy transfer, were limited by the crossing angle between pump and seed. Gains were most often *relative*: the transferred energy compensated only partially the propagation-induced losses in the plasma. That was a proof-of-principle experiment, the transition into the self-similar regime and its consequences on the amplified seed (pulse duration, frequency spectrum, amplification length) were not studied, nor the Raman and Brillouin interplay. In the following, we report on the first observation of the signatures of the transition from linear to self-similar regimes of SC-SBA, so far only predicted by theory and simulations [13,24]. With a new fully head-on collision geometry, subpicosecond pulses are amplified by a factor of 5 with energy transfers of few tens of mJ. We observe pulse shortening, frequency spectrum broadening, and down-shifting for increasing gain, signatures of SC-SBS amplification entering the self-similar regime. This is also confirmed by the power law dependence of the gain on the amplification length: doubling the interaction length increases the gain by a factor 1.4. Pump backward Raman scattering (BRS) on SC-SBA has been measured for the first time, showing a strong decrease of the BRS amplitude and frequency bandwidth when SBS seed amplification occurs. The experimental results also show the higher efficiency of the head-on collision geometry compared to the previous crossed geometry [17]: *absolute* gains and similar pump energy transfers of few tens of mJ into subpicosecond pulses are obtained despite pump and seed intensities, respectively, 30 and 170 times lower.

The growth rate $\Im(\omega_{SC})$ for SC-SBS amplification of the seed pulse depends [cf. Eq. (1)] on the product $n_e I$. In a head-on collision geometry, due to the longitudinal profiles of both plasma density $n_e(z)$ and pump intensity $I(z,t)$, a crucial parameter is the relative delay $\Delta t = t_p - t_s$ between pump and seed arrival at the plasma center. Calculated from Eq. (1) (square bracket) with experimental parameters detailed below, the growth rate seen by the seed along its propagation axis z, and for different delays Δt, is shown in Fig. 1. A change in Δt not only shifts the position where the maximum coupling occurs, it also strongly affects the amplitude of this maximum. For example, when $\Delta t = -6$ ps (green solid curve), the pump arrives at the plasma center before the seed. The growth rate reaches its maximum at $z = -0.4$ mm (before the peak of the plasma density) with a value $\gamma_{SC}/\omega_0 \approx 0.08$, lower than at $\Delta t = 0$ ps. One can thus explore the pump-seed coupling from linear to self-similar regimes, while keeping the same plasma and laser parameters (focal spot size, laser energy, pulse duration), and avoid triggering or modifying other limiting mechanisms such as beam filamentation or wave breaking [22].

The experiment has been performed at LULI on the ELFIE facility. Three CPA pulses, of wavelength $\lambda_0 = 1058$ nm (~6 nm FWHM bandwidth), were used: a pump, a seed, and an ionizing beam, this last one generating the plasma from a supersonic hydrogen gas jet. A fully counterpropagating geometry between pump and seed was set up in order to maximize the interaction length, only limited by plasma length. The 4 mJ–0.7 ps (FWHM) seed was focused to 130 μm (FWHM), leading to a maximum intensity of

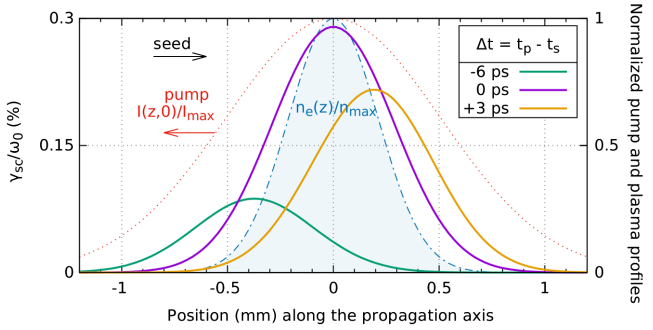

FIG. 1. Evolution of the growth rate (solid curves, left scale) $\gamma_{SC} = \Im(\omega_{SC})$ seen by the seed along its propagation (left to right), and for different delays Δt with the counterpropagating pump (dotted red curve, right scale). At $\Delta t = 0$ the pulses cross at $z = 0$, in the middle of the plasma profile (blue area with dash-dotted curve, right scale). Calculated from Eq. (1) with experimental parameters (H_2, $I_{15} = 1$, $n_e = 0.1 n_c$).

3×10^{13} W/cm^2. The 6 J pump was focused to 150 μm (FWHM) in order to spatially overlap the seed. To cover the whole interaction length, the pump was stretched to 4 ps (positive frequency chirp, ~1.5 nm/ps), leading to a maximum intensity of 2×10^{15} W/cm^2. The ionizing beam was an uncompressed 450 ps chirped pulse of 30 J. To fully ionize the whole pump-seed interaction region it was focused to a large elliptical focal spot with a hybrid phase plate. The ionizing pulse was sent 1.5 ns before pump and seed pulses, in order to let the plasma hydrodynamics smooth the small-scale (μm) inhomogeneities. The plasma density profile was Gaussian with a 0.5 mm FWHM along the propagation axis (represented by the blue dash-dotted curve in Fig. 1). Maximum plasma density was adjusted between 0.05 and $0.17 n_c$ by changing the gas jet backing pressure. At the highest value ($n_e = 0.17 n_c$) and for $I_{15} = 2$, the SC-SBS growth rate is $\gamma_{SC}/\omega_0 \simeq 4.6 \times 10^{-3}$, corresponding to a typical growth time of the order of 120 fs, a few times faster than the seed duration. For the results presented in the following, using the measured gas jet profile and ionizing beam parameters, hydrodynamic simulations predict an electron (ion) plasma temperature of T_e (T_i) $\simeq 100(90)$ eV. For these plasma parameters and $\lambda_0 = 1058$ nm the strongly coupled regime is reached at $I > 3 \times 10^{12}$ W/cm^2 [21].

The energies of the transmitted pump and seed were measured by focusing the beams at the plasma exit onto 16 bit Si charge coupled devices (CCDs). The light at the seed exit was also sent to a second-order autocorrelator in order to discriminate possible contributions of the pump SBS (long pulse), from the actual energy transfer to the short seed. The frequency spectrum of this light was also analyzed (i) with a high resolution spectrometer, coupled to a 16 bit Si CCD, to measure the transmitted (amplified) seed spectrum, and (ii) with a low-resolution spectrometer, coupled to an IR 12 bit InGaAs CCD, to measure the backward Raman spectrum of the pump. In addition to these beam diagnostics, the plasma was probed by a 0.5 ps pulse, coupled to a Nomarski interferometric diagnostic; this allowed monitoring the global symmetry and homogeneity of the plasma profile.

To find the best conditions for an efficient beam coupling, the energies, spectral and temporal characteristics of the transmitted beams, as well as pump backscattered light, were analyzed by varying laser, plasma, and interaction parameters. We present in Fig. 2 the seed energy gain (blue circles, left scale) and the backscattered Raman energy from the pump into the seed propagation direction (green squares, right scale), as a function of Δt. The uncertainty on the absolute zero timing is of the order of 1.5 ps. The relative uncertainty in time between points is of the order of ± 30 fs. The energy gain is defined as the ratio between the signal at the seed exit of the plasma, and the signal of the seed propagating in vacuum, both normalized to the seed incident energy, recorded by a calibrated photodiode. Two types of gain measurement are shown: they are obtained from the

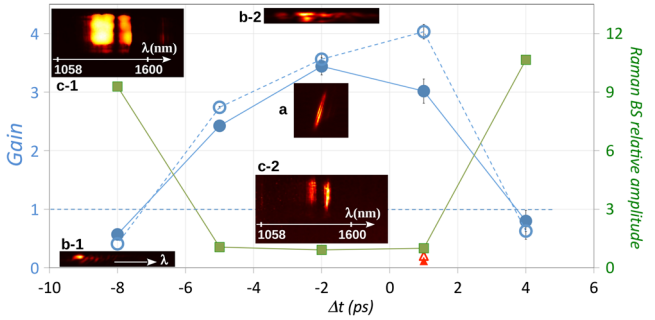

FIG. 2. Energy gain E_{out}/E_{in} of the seed (left scale, blue circles) and pump Raman backscattered signal (right scale, green squares), as a function of relative delay between pump and seed arrival time at the plasma center. Full (empty) circles are the 2D (1D) calorimetry. Plasma density is 0.1 n_c. Gain = 1; dashed line is the level of incident light. The level of seed transmission without pump is represented by red triangles. Raman signal is normalized to its value at the $\Delta t = 0$ ps delay. The insets illustrate typical raw data for each diagnostics: 2D calorimetry (a), 1D calorimetry, i.e., seed spectrum (b-1 and b-2), Raman spectrum (c-1 and c-2).

integration (i) of the CCD images of the focal spot (2D calorimetry, full circles) and (ii) of the spectrum (1D calorimetry, empty circles). For the 1D calorimetry only a vertical slice of the focal spot is selected through the spectrometer slit. A good agreement is observed between these two measurements, indicating that the energy transfer occurs in the spectral bandwidth of the seed. The slightly higher gain, recorded from the 1D calorimetry, suggests that a higher amplification occurs in the central part of the beam, i.e., the one selected by the spectrometer slit. Without pump, the seed is attenuated along its propagation through the plasma down to a transmission level of 10% (red triangles). Note that, compared to previous measurements [17], performed with an Ar gas jet, the use of H_2 allowed one to fully ionize the interaction volume and reduce small density gradients, increasing the seed transmission by a factor 10–50.

The gain asymmetry with respect to the zero delay can be explained as follows: at positive delays, the seed propagates in the plasma (therein undergoing attenuation and perturbations) before interacting with the high intensity part of the pump; this slows down the amplification process. On the opposite, at negative delays, an unperturbed seed starts interacting with the most intense part of the pump, so that the self-similar SC-SBA regime is more easily reached. Even if the gain factors at $\Delta t = -8$ ps and $+4$ ps are lower than one, they are higher than the case without pump. This indicates that even the low efficiency interaction results from the two beams coupling.

Stimulated Raman scattering could reduce the efficiency or quality of the Brillouin amplification process [25]. For very short pulses it could also contribute to the seed amplification [21]. Using a low-resolution spectrometer coupled to an IR camera, we measured for the first time the spectrum of backward Raman scattering (BRS) from the pump into the seed direction. Two typical BRS spectra are

presented as insets in Fig. 2. The BRS energy, obtained by spectral integration in the 1100–1700 nm range and spatial integration along the spectrometer slit axis, is also presented in Fig. 2 (green squares, right scale). At higher values of seed energy gain, the BRS signal has a lower amplitude and frequency bandwidth with respect to shots at lower gain. This can be attributed to the ionlike density fluctuations that affect the evolution and saturation of Langmuir waves, and quench stimulated Raman scattering (SRS) [26]. One-dimensional particle-in-cell (PIC) simulations were performed with the code SMILEI [27], using the experimental laser-plasma parameters. They show a narrowing of the BRS spectrum and a ~10 times weaker BRS energy when SC-SBA occurs, in very good agreement with our measurements (insets and green squares). The anticorrelation shown in the figure is to be interpreted as further proof of successful seed amplification by SC-SBS energy transfer.

As previously stated, the agreement between 2D and 1D calorimetry (spectrum), shown in Fig. 2, allowed us to infer that the pump energy is transferred within the spectral bandwidth of the seed. However, this does not demonstrate that the seed is in fact amplified, as, for this to be true, the pump energy must be transferred within the seed temporal envelope. By Gaussian fitting ($Ae^{-(t/\tau_a)^2}$) the autocorrelation trace [28], one can retrieve the pulse duration $\tau = \tau_a/2^{1/2}$, its relative intensity $I \propto A^{1/2}$ (in arbitrary units), hence its relative energy τI. In this way the second-harmonic autocorrelator diagnostic provides, together with the measurement of the pulse duration, an estimate of the energy gain. This is shown in Fig. 3 where, for the same data set of Fig. 2, the retrieved duration is represented by triangles and the energy gain by circles. We observe that pulse duration is minimal at the maximum gain and close to the vacuum seed duration. Moreover, the energy gain is in very good agreement with the one measured from 2D calorimetry. These coupled results demonstrate that pump energy is indeed transferred into the seed, and the realization of a subpicosecond laser pulse single pass plasma amplifier. At intermediate negative delays interaction starts with the high intensity part of the pump and thus reaches the self-similar regime: a fast growth rate is set, associated to a large spectral amplification bandwidth, leading to a short pulse duration. At large negative delays, the high intensity part of the pump leaves the plasma before the seed arrival. Interaction occurs in the linear regime with a slow growth rate and the weakly amplified seed becomes longer [24]. This is also the case for intermediate positive delays since the seed mostly interacts with the low intensity rising edge of the pump. Let us note that without seed no autocorrelation trace was detected. It results only from the pump and seed electromagnetic coupling [29].

The correlation between the output pulse duration and the amplification bandwidth is observed on the amplified seed spectra. Figure 4(a) shows the transmitted seed spectra, expressed in spectral energy density (mJ/nm), for the different pump-seed delays. It corresponds to the same data set of Figs. 2 and 3. We observe that at large delays the seed is weak (low gain) with a narrow spectrum, and that the larger the gain the larger the spectral bandwidth. Moreover, an important observed correlated feature is that at increasing gain the spectrum redshifts more. Since the growth rate $[\Im(\omega_{SC})]$ and the ion mode frequency $[\Re(\omega_{SC})]$ increase with laser intensity [Eq. (1), $\omega_{SC} \propto I^{1/3}$], the amplified seed should indeed present a broader and more redshifted spectrum at larger gain. At the peak of the density profile ($n_e/n_c = 0.1$) and pump intensity (10^{15} W/cm^2) Eq. (1) gives a maximum redshift of 0.17%; i.e., for $\lambda_0 = 1058$ nm a spectrum peaked at ~1060 nm, in very good agreement with the experimental result at maximum gain (blue curve, $\Delta t = +1$ ps). Further comparison with theory requires taking into account pump, seed, and plasma evolution. Transmitted spectra obtained from 1D-PIC simulations, using the experimental laser-plasma parameters, are shown in Fig. 4(b). They represent the Fourier transforms of the seed electric field after interaction, for two different pump-seed delays. The spectrum is only shown over the interval of interest. As experimentally observed, at the delay t_{opt} giving the maximum amplification, also correspond the largest

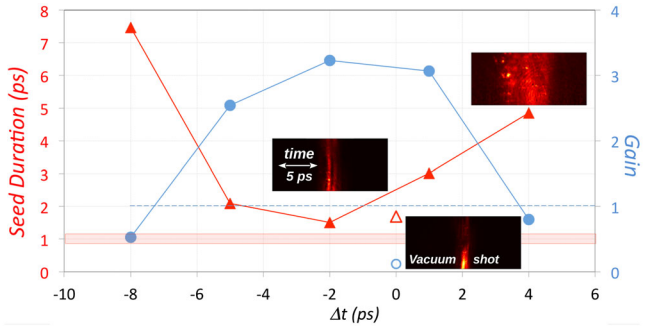

FIG. 3. Duration (FWHM, left axis, triangles) and energy gain (right axis, circles) of the transmitted light evaluated from a Gaussian fit of the autocorrelation trace. Same data set of Fig. 2. The width of the red band shows the amplitude of shot to shot fluctuations on the incident seed duration. The empty triangle (circle) is the seed duration (gain) without pump. The insets illustrate typical raw data.

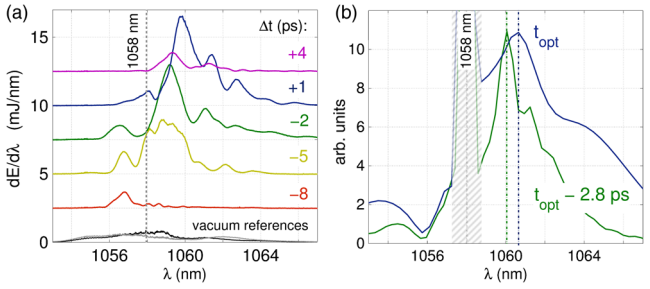

FIG. 4. (a) Transmitted spectra, expressed in mJ/nm, as a function of the delay. Two reference spectra in vacuum propagation are shown. Same data set of Figs. 2 and 3. (b) 1D-PIC simulated spectra: optimal case (blue solid line) and delayed (green). The peak at the initial pump and seed wavelength (1058 nm) is masked to show only the spectra related to the amplification process.

redshift and spectral width. Both the amplitude of the redshift and the spectral broadening are in relatively good agreement with the experiment. As the 1D-PIC simulation accounts for all possible kinetic and nonlinear effects, the residual differences are attributed to 2D-3D geometry effects, pump frequency chirp, or uncertainties in plasma and laser characterization.

To investigate the optimization of the process in terms of interaction length, we used a longer plasma (1 mm FWHM, Gaussian profile) with the same maximum plasma density ($0.1n_c$). To match the plasma length, the pump duration was set to 6 ps, while keeping its intensity the same (increasing its energy to 9 J). In these conditions, the energy and intensity of the seed pulse were amplified up to a factor of 5, meaning ~30 mJ of energy transfer. Correlated to this larger amplification factor, we observed a larger frequency shift of ~0.28% of the seed spectrum. By keeping the same laser parameters and using lower plasma density, we observed that both the frequency shift and the spectral bandwidth reduce, in agreement with the fact that ω_{SC} decreases with plasma density [cf. Eq. (1)].

In conclusion, we have reported on the first observation of the signatures of the transition from linear to self-similar regimes of SC-SBA, so far only predicted by theory and simulations. We observed pulse shortening, frequency spectrum broadening, and down-shifting for increasing gain, signatures of SC-SBS amplification entering the self-similar regime. This is also confirmed by the power law dependence of the gain on the amplification length: by doubling the interaction length, the energy and intensity gain increases by a factor of 1.4. A strong decrease of the BRS when SBA occurs has been measured for the first time. PIC simulations corroborate these findings, further indicating that SBS is responsible for the amplification, strongly limiting the growth of SRS.

F. Amiranoff and P. Loiseau are acknowledged for fruitful discussions. The ELFIE technical team is gratefully acknowledged. L. L. benefited from support of CRISP FP-7 Contract No. 283745. S. W. benefited from the support of ELI-Beamlines (Project No. CZ.1.05/1.1.00/02.0061). C. R. and M. C. acknowledge support from Grant No. ANR-11-IDEX-0004-02 Plas@Par. The authors want to thank the SMILEI development team and Maison de la Simulation for support and granting them access to their in-house supercomputer Poincaré. This work has been partially funded by LASERLAB-EUROPE (Grant Agreement No. 284464, EC's Seventh Framework Program).

*Corresponding author.
livia.lancia@uniroma1.it

[1] R. D. Milroy, C. E. Capjack, and C. R. James, Phys. Fluids **22**, 1922 (1979).
[2] J. Fuchs, A. A. Gonoskov, M. Nakatsutsumi, W. Nazarov, F. Quéré, A. M. Sergeev, and X. Q. Yan, Eur. Phys. J. Spec. Top. **223**, 1169 (2014).
[3] A. Di Piazza, C. Müller, K. Z. Hatsagortsyan, and C. H. Keitel, Rev. Mod. Phys. **84**, 1177 (2012).
[4] B. C. Stuart, M. D. Feit, A. M. Rubenchik, B. W. Shore, and M. D. Perry, Phys. Rev. Lett. **74**, 2248 (1995).
[5] D. Strickland and G. A. Mourou, Opt. Commun. **56**, 219 (1985).
[6] A. Dubietis, G. Jonušauskas, and A. Piskarskas, Opt. Commun. **88**, 437 (1992).
[7] V. M. Malkin, G. Shvets, and N. J. Fisch, Phys. Rev. Lett. **82**, 4448 (1999).
[8] J. Ren, W. Cheng, S. Li, and S. Suckewer, Nat. Phys. **3**, 732 (2007).
[9] Y. Ping, W. Cheng, S. Suckewer, D. S. Clark, and N. J. Fisch, Phys. Rev. Lett. **92**, 175007 (2004).
[10] W. Cheng, Y. Avitzour, Y. Ping, S. Suckewer, N. J. Fisch, M. S. Hur, and J. S. Wurtele, Phys. Rev. Lett. **94**, 045003 (2005).
[11] Z. Toroker, V. M. Malkin, and N. J. Fisch, Phys. Plasmas **21**, 113110 (2014).
[12] M. R. Edwards, Z. Toroker, J. M. Mikhailova, and N. J. Fisch, Phys. Plasmas **22**, 074501 (2015).
[13] A. A. Andreev, C. Riconda, V. T. Tikhonchuk, and S. Weber, Phys. Plasmas **13**, 053110 (2006).
[14] A. Frank *et al.*, Eur. Phys. J. Spec. Top. **223**, 1153 (2014).
[15] E. Guillaume *et al.*, High Power Laser Sci. Eng. **2**, e33 (2014).
[16] K. A. Humphrey, R. M. G. M. Trines, F. Fiuza, D. C. Speirs, P. Norreys, R. A. Cairns, L. O. Silva, and R. Bingham, Phys. Plasmas **20**, 102114 (2013).
[17] L. Lancia, J. R. Marquès, M. Nakatsutsumi, C. Riconda, S. Weber, S. Hüller, A. Mančic, P. Antici, V. T. Tikhonchuk, A. Heron, P. Audebert, and J. Fuchs, Phys. Rev. Lett. **104**, 025001 (2010).
[18] G. Lehmann, F. Schluck, and K. H. Spatschek, Phys. Plasmas **19**, 093120 (2012).
[19] G. Lehmann, and K. H. Spatschek, Phys. Plasmas **20**, 073112 (2013).
[20] C. Riconda, S. Weber, L. Lancia, J.-R. Marquès, G. A. Mourou, and J. Fuchs, Phys. Plasmas **20**, 083115 (2013).
[21] C. Riconda, S. Weber, L. Lancia, J.-R. Marquès, G. Mourou, and J. Fuchs, Plasma Phys. Controlled Fusion **57**, 014002 (2015).
[22] S. Weber, C. Riconda, L. Lancia, J. R. Marquès, G. A. Mourou, and J. Fuchs, Phys. Rev. Lett. **111**, 055004 (2013).
[23] D. W. Forslund, J. M. Kindel, and E. L. Lindman, Phys. Fluids **18**, 1002 (1975).
[24] G. Lehmann, and K. H. Spatschek, Phys. Plasmas **22**, 043105 (2015); F. Schluck, G. Lehmann, and K. H. Spatschek, Phys. Plasmas **22**, 093104 (2015).
[25] R. Trines *et al.*, arXiv:1406.5424v1.
[26] H. A. Baldis, P. E. Young, R. P. Drake, W. L. Kruer, K. Estabrook, E. A. Williams, and T. W. Johnston, Phys. Rev. Lett. **62**, 2829 (1989).
[27] http://www.maisondelasimulation.fr/projects/Smilei/html/index.html.
[28] A. Brun, P. Georges, G. Le Saux, and F. Salin, J. Phys. D **24**, 1225 (1991).
[29] As in the previous experiment [17] a polarization test systematically confirmed electromagnetic coupling, showing a lower (but not zero) energy transfer for crossed polarizations. Because of the higher efficiency of the head-on geometry, the energy transfer was not zero: a residual parallel polarization component was enough to trigger a non-negligible energy transfer.